FARADAY

Hydrogen electrochemistry on platinum low-index single-crystal surfaces in alkaline solution

Nenad M. Marković,* Stella T. Sarraf, Hubert A. Gasteiger† and Philip N. Ross, Jr.
Materials Sciences Division, Lawrence Berkeley National Laboratory, University of California Berkeley, CA 94720, USA

The results of a study of the hydrogen evolution reaction (HER) and the hydrogen oxidation reaction (HOR) on the three low-index faces of Pt in alkaline solution are presented. The study features a new method for the use of Pt single crystals in a rotating disk electrode (RDE) configuration. At low negative overpotentials, the order of activity for the HER increased in the sequence (111) < (100) < (110). At low positive overpotentials, the order of activity for the HOR increased in the sequence (111) ≈ (100) ≪ (110). These differences in activity with crystal face are attributed to different states of adsorbed hydrogen and to different effects of these states on the mechanism of the hydrogen reaction. Two different types of adsorbed hydrogen are observed on Pt(*hkl*) surfaces. A high binding energy state, often referred to as underpotential deposited hydrogen, H_{upd}, has an inhibiting (site blocking) effect on the rate of the HER and HOR. A low binding energy state is a reaction intermediate at low overpotentials in both the HOR as well as the HER, and is most prevalent on the (110) surface. At high positive overpotentials, in the potential region where adsorption of hydroxy species (OH_{ad}) occurs, the effects of surface crystallography on the HOR is attributed to the structural sensitivity of the adsorption of OH_{ad} on Pt(*hkl*), with OH_{ad} having an inhibiting effect on the HOR, the inhibition decreasing in the sequence (100) ≪ (110) < (111).

1. Introduction

The hydrogen reaction is one of the most extensively investigated electrochemical processes. All the basic laws of electrode kinetics as well as the modern concepts for electrocatalysis study were developed and verified by examining the hydrogen evolution (HER) and the hydrogen oxidation (HOR) reactions.[1,2] Nearly five decades ago the hydrogen reaction served as a model to establish an empirical volcano relationship between the electrocatalytic rate (expressed as the exchange current densities, i_0) and the substrate electronic properties.[3] So-called 'volcano plots' correlating the exchange current density with changes of standard Gibbs energy of adsorption of hydrogen ($\Delta_{ad}G$) have been rationalized by Parsons,[4] Gerischer,[5] and Kristhalik[6] in terms of various possible reaction steps for different metal electrodes. Somewhat later empirical volcano plots by Trasatti[7,8] appeared to support these analyses. For constructing volcano plots $\Delta_{ad}G$ was inferred from gas-phase data in low pressure conditions and Pt was classified among the group of metals with $\Delta_{ad}G < 0$. Protopopoff and Marcus,[9] however, suggested that Pt should be correlated with the gas-phase data for dissociative adsorption of H_2 under high pressure conditions (since the HER begins at an equivalent pressure of *ca.* 1 atm), and therefore Pt should be classified among the group of metals with $\Delta_{ad}G > 0$. Nevertheless, regardless of the position of Pt in the volcano curve, these correlations do not provide answers to many important questions concerning the mechanism of the hydrogen reaction on Pt. For example, what is the relationship between the adsorbed hydrogen produced during the HER (Conway and others have called this species overpotential hydrogen, H_{opd}) and the adsorbed hydrogen produced in the underpotential region (H_{upd})? What is the role of both H_{upd} and H_{opd} in the mechanism of the HER? What is the role of H_{upd} in the mechanism of the HOR at different overpotentials and under different experimental conditions, especially at different pH? As pointed out by Bagotzky and Osetrova,[10] a strong dependence of the kinetics of the HOR on pH poses a fundamental problem for the most frequently proposed mechanism for the HOR on Pt, the Tafel–Volmer sequence with the Tafel step as rate determining.[1] Certainly, it will be difficult, if not impossible, to resolve all of these mechanistic details by studying the reaction on a heterogeneous surface, such as the polycrystalline Pt electrodes used in nearly all previous kinetic studies. Thus, a knowledge of the effects of the surface structure on the rate of the HER and HOR will play an essential role in illuminating the fine details of the hydrogen reaction.

Kinetic studies of the HER on Pt single-crystal electrodes have been reported in acid solution[11–13] and no effect of orientation was found. The significance of these results is, however, questionable since it is not clear that true kinetic rates were actually measured in any of these studies. As emphasized by Bagotzky and Osetrova,[10] and much earlier by Breiter *et al.*,[14] the hydrogen reaction on 'active' Pt in acidic solutions is one of the fastest known electrochemical reactions (with an $i_0 \gg 10^{-3}$ A cm^{-2}), and it is experimentally very difficult to measure anything but diffusion polarization. Therefore, in our opinion it is experimentally very difficult to correlate the rate of the reaction in acid solution with the surface geometry, even if indeed the kinetics were dependent on the crystallographic orientation of Pt(*hkl*). In an alkaline electrolyte, however, the rate of the HER and HOR on a polycrystalline electrode is reduced by more than one order of magnitude from that in acid solution, and the accurate measurement of kinetic rates appears more tractable.

In this report, we present results for the kinetics of both the HER and HOR in alkaline solution, utilizing the rotating disk [$RD_{Pt(hkl)}E$] technique we employed in our recent study of the oxygen reduction reaction (ORR) on Pt(*hkl*) in 0.1 M KOH.[15,16] A striking structural sensitivity of the kinetics of both the HER and HOR is seen on Pt(*hkl*) in 0.1 M KOH. We present an analysis of the kinetic data which shows that hydrogen adsorbed in the underpotential region (H_{upd}) have inhibiting (site blocking) effects on the HER and HOR on

† Present address: Abt. für Oberflächenchemie und Katalyse, Universität Ulm, D-89069 Ulm, Germany.

Pt(*hkl*), which sharply contrast with the behaviour observed in acid solution. We also present an analysis of the role of adsorbed hydroxy species (OH_{ad}) in the kinetics of the HOR on Pt(*hkl*).

2. Experimental

The pretreatment and assembling of the Pt(*hkl*) single crystals (0.283 cm^2) in an $RRD_{Pt(hkl)}E$ configuration was fully described in our previous paper. Following flame annealing, the single crystal was mounted in the disk position of an insertible ring disk electrode assembly.[15] Subsequently, it was transferred into a standard electrochemical cell and immersed into 0.1 M KOH (J. T. Baker Reagent) under potentiostatic control at *ca.* 0.2 V. The cleanliness of the transfer and the electrolyte, even under sustained rotation at high rotation rates, were demonstrated in our previous work.[15] Upon immersion, the electrolyte was equilibrated for 5 min with the hydrogen gas (Spectra Gases, 6N). All measurements were conducted at room temperature, *ca.* 25 °C. All potentials are referenced to the reversible hydrogen electrode (RHE) at 1 atm hydrogen in the same electrolyte. Current–potential curves were obtained potentiodynamically and were recorded simultaneously on a chart recorder and digitally on an IBM PC (486) computer using Labview for Windows.

3. Results

3.1 Cyclic voltammograms of Pt(*hkl*) in 0.1 M KOH

Comparison of the cyclic voltammograms of Pt(*hkl*) electrodes in hydrogen-free 0.1 M KOH is shown in Fig. 1. The interpretation of the voltammetry of Pt(*hkl*) in alkaline electrolyte has been discussed in our recent paper.[16] For continuity, we present a brief summary of that interpretation here. Only on

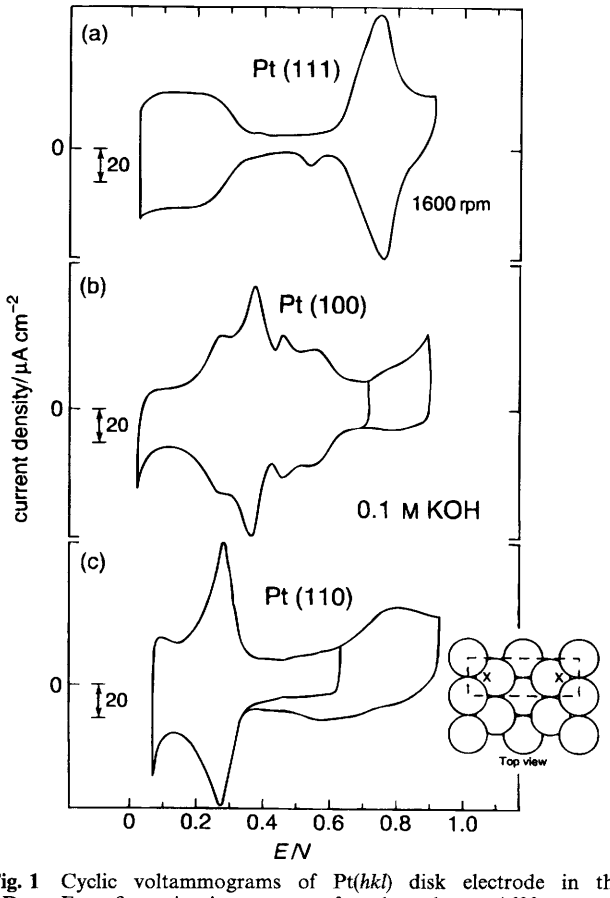

Fig. 1 Cyclic voltammograms of Pt(*hkl*) disk electrode in the $RD_{Pt(hkl)}E$ configuration in an oxygen-free electrolyte at 1600 rpm and a sweep rate of 50 mV s^{-1}

Pt(111) is hydrogen adsorption separated in potential from the adsorption of hydroxy anions by a true double-layer potential region. A distinguishing characteristic of both the Pt(100) and Pt(110) single crystals in 0.1 M KOH is that a true double-layer potential region does not exist on these surfaces. For both the (100) and (110) surfaces, on the positive-going sweep the desorption of hydrogen is immediately followed by the adsorption of oxygen-like species, for simplicity we shall call these species OH_{ad}. On (100), these processes actually overlap, with OH_{ad} forming on some parts of the surface while H_{upd} is still present on other parts. Two different types of OH_{ad} can be distinguished on the Pt(100) electrode; a reversible form of hydroxy species, which is formed within a potential region $0.45 < E/V < 0.7$, and an irreversible form of hydroxy species formed at more positive potentials, $E > 0.7$ V. In the case of (110), the hydrogen desorption ($0.05 < E/V < 0.35$) is also followed by the reversible adsorption of OH_{ad} ($0.35 < E/V < 0.65$) and then by the formation of an irreversible form of OH_{ad}. While the exact nature of these two forms is not known, we have postulated that the difference between the reversible and irreversible forms of OH_{ad} is the coordination with Pt. The reversible form is adsorbed onto the outermost plane of Pt atoms as partially (or fully) discharged OH_{ad} anions as in

$$OH^- + \delta e^- \rightleftharpoons OH_{ad}^{-(1-\delta)} \quad (1)$$

while the irreversible form is in or below the outermost plane of Pt atoms, probably by place-exchange with Pt surface atoms. The nature, as well as the surface coverage, of both H_{ad} and OH_{ad} species are expected to play an important role in the kinetics of hydrogen reaction on Pt(*hkl*), as discussed below.

A detailed description of our procedure for the determination of the charge associated with both underpotential deposited hydrogen (H_{upd}) and the adsorption of hydroxy species (OH_{ad}) on Pt(*hkl*) in alkaline solution as a function of electrode potential has been discussed in our recent publication.[16] Briefly, the accuracy of the charge integration from the voltammograms of Fig. 1 is dependent primarily upon two possible sources of error. One involves the method of correction for the double-layer capacitance, and the other, with the exception of the Pt(111) plane, involves uncertainty in the deconvolution of the charge associated with H_{upd} from the charge corresponding to OH_{ad}. In this work, as in ref. 16, the capacitance of the Pt(*hkl*)–solution interface was determined from the Pt(111) curve by assuming that the current in the potential region $0.35 < E/V < 0.65$ is indicative of a 'true' double-layer charging current for all Pt surfaces. The procedure for deconvoluting $Q_{H_{upd}}$ from $Q_{OH_{ad}}$ on Pt(100) and Pt(110) was trial-and-error curve fitting of the voltammetry curves such that the charge from integrating the current on the positive-going sweep from $0.05 > E/V > 0.5$ gives the number of coulombs required to remove a monolayer of adsorbed hydrogen adatoms from these two surfaces. The fractional coverage, θ, for either H_{upd} or OH_{ad} is based on the surface atomic density assuming one-electron transfer per surface atom. The surface atomic densities for (111) and (100) were based on their unreconstructed (1 × 1) geometry rather than any reconstructed phase because our recent surface X-ray scattering (SXS) studies confirmed the (1 × 1) structure of the Pt(111) (1.5×10^{15} atoms cm^{-2}) and Pt(100) (1.3×10^{15} atoms cm^{-2}) single crystals in contact with several electrolytes.[17,18] SXS results for Pt(110) have indicated that, in the potential region relevant to this work, Pt(110) is reconstructed into a (1 × 2) structure with a surface density of 4.6×10^{14} atoms cm^{-2}.[19] The (1 × 2) geometry involves a change of 50% in the surface atomic density, in comparison with the (1 × 1) surface, since every other row is missing, as shown in the insert of Fig. 1(c). The theoretical charge for the formation of the monolayer of H_{upd} and OH_{ad} on the (1 × 1)

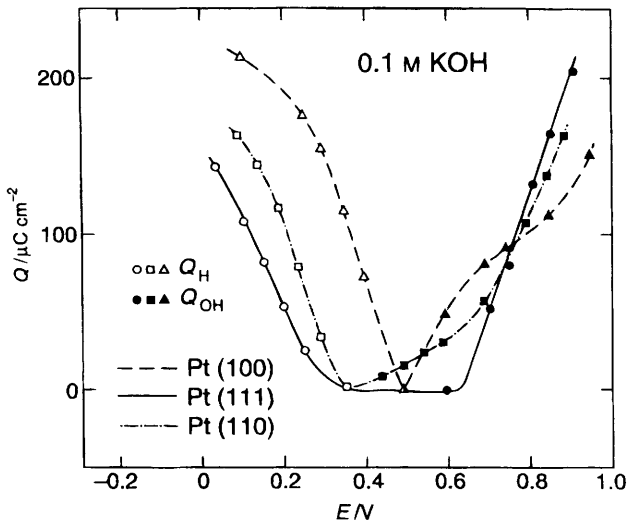

Fig. 2 Plots of the charge associated with the underpotential deposition of hydrogen (H_{upd}) and adsorption of hydroxy species (OH_{ad})

and (1 × 2) surfaces, however, is the same (*ca.* 147 μC cm^{-2}) since two H_{upd} or OH_{ad} species can be adsorbed per unit cell of the reconstructed Pt(110) (1 × 2) surface [indicated by the letter X in the top view of the surface in Fig. 1(c)]. Adsorption of hydrogen into these sites was proposed as the mechanism for an increase in corrugation of the Pt(110) surface in both UHV[20] and *in situ* X-ray scattering measurements.[19] The resulting isotherms for H_{upd} and OH_{ad} are shown in Fig. 2.

3.2 Hydrogen evolution reaction (HER)

Polarization curves over a wide range of overpotentials, both anodic and cathodic, for the hydrogen reaction at 1 atm on rotating Pt(*hkl*) disk electrodes are shown in Fig. 3. On the cathodic side, only a weak dependence of current density on the rotation rate was observed on all three single crystal surfaces. This is most likely due to H_2 diffusion effects, *i.e.*, a supersaturation by H_2 and its influence on the overpotential, as discussed by Breiter *et al.*,[21] Ludwig *et al.*[22] and Conway and Bai.[23] Very reproducible current *vs.* potential relationships, however, were established at a rotation rate of 3600 rpm and higher, indicating that at and above 3600 rpm the supersaturation effect by molecular H_2 is practically eliminated. Polarization curves at 3600 rpm for all three surfaces are compared in Fig. 4. This comparison clearly shows that the activity for the HER on Pt(*hkl*) increases in the sequence (111) ≪ (100) < (110).

3.3 Hydrogen oxidation reaction (HOR)

In the polarization curves for Pt(111) in Fig. 3(a), there is little or no rotation rate dependence to the current at low anodic overpotentials, implying entirely kinetic resistance of the HOR up to about +0.05 V. At higher overpotentials, however, the HOR is under mixed kinetic–diffusion control, and above +0.5 V well defined diffusion-limiting currents, *i.e.*, $i \propto \omega^{0.5}$ were observed, indicating the HOR is purely controlled by the mass transport of molecular H_2 at $E > +0.5$ V. Interestingly, and significantly as we see later, the diffusion limiting currents were also observed while the potential was swept across the potential region where the electrode has a relatively high coverage by OH_{ad} (Fig. 2).

The anodic polarization curves for the (100) surface [Fig. 3(b)] have both similar and contrasting character to the (111) surface. As in the case of Pt(111), at low overpotentials there is little or no rotation dependence out to about +0.05 V, but true diffusion limiting currents are observed only in a very

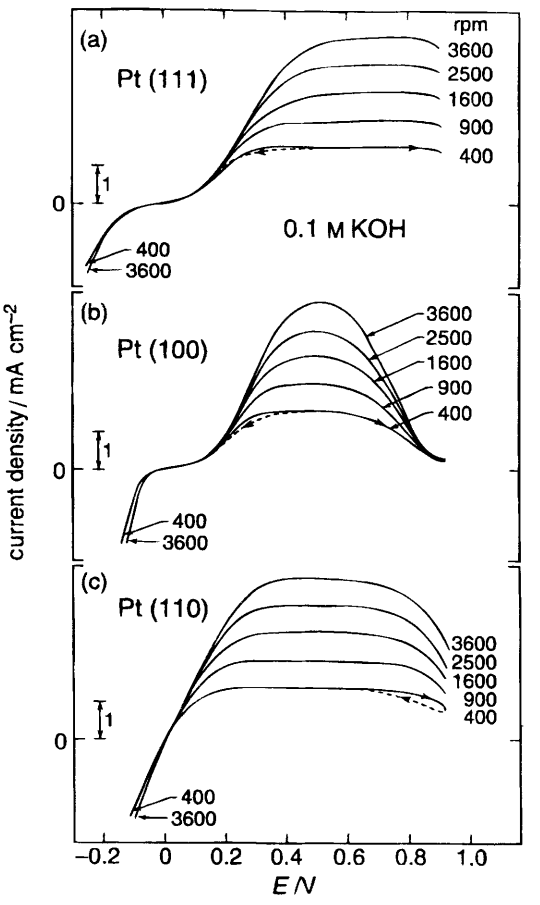

Fig. 3 Polarization curves for the HER and HOR on Pt(*hkl*) in 0.1 M KOH at a sweep rate of 20 mV s^{-1}

narrow potential region, between *ca.* 0.55 and 0.6 V. Unlike (111), above 0.6 V the activity of the (100) surface declines precipitously as the potential is scanned through the region of OH_{ad} formation (see Fig. 2), which implies that OH_{ad} species have an inhibiting effect (site blocking) on the kinetics of the HOR on this surface. An analogous phenomenon was observed many years ago† for polycrystalline Pt in acid electrolyte, and was rationalized then as the effect of the formation of surface 'oxide' on the kinetics of the HOR.

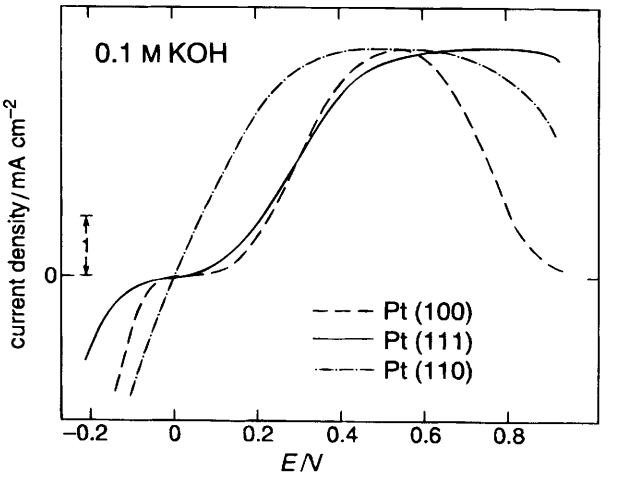

Fig. 4 Polarization curves for the HER and HOR on Pt(*hkl*) in 0.1 M KOH at 3600 rpm

† See ref. 1, pp. 550–551 for a complete historical account.

Our results for the HOR on Pt(110) [Fig. 3(c)] are quite similar to those reported in the literature, *e.g.*, Bagotzky and Osterova,[10] for a polycrystalline Pt electrode in either 0.1 M KOH or NaOH. Diffusional resistance appears at very low overpotential, *e.g.*, tens of mV, indicating a much higher exchange current density for this surface than for the other two. Unlike the other two surfaces, this high activity occurs on a surface with a high coverage of H_{upd}, indicating that, for Pt(100), H_{upd} is not a self-inhibiting intermediate. Above 0.7 V the increasingly higher coverage by OH_{ad}, which in this potential region is mostly of the irreversible form, does appear to inhibit the reaction.

3.4 Kinetic analysis

In strong contrast to the behaviour in acid solution, the HOR on Pt(111) and (100) in alkaline solution is purely kinetically controlled over a relatively wide potential region, even at rotation rates as low as 400 rpm. It is under mixed control up to *ca.* 0.4 V of overpotential. On the (110) surface, the currents are under mixed control up to *ca.* 0.2 V of overpotential, providing a relatively wide window of overpotential where kinetic analysis can be performed by using the Levich–Koutecky equation,

$$\frac{1}{i} = \frac{1}{i_k} + \frac{1}{i_d} = \frac{1}{i_k} + \frac{1}{c_0 B\omega^{-0.5}} \qquad \text{(I)}$$

where i_k is the kinetically controlled current density, and i_d is the mass-transport limited current density

$$i_d = 0.62\, nFD^{2/3}\nu^{-1/6}c_0\,\omega^{1/2} = Bc_0\,\omega^{1/2} \qquad \text{(II)}$$

in which nF is the charge transferred per mole, D is the diffusion coefficient, c_0 is the solubility of H_2 and ν is the kinematic viscosity of the electrolyte. Fig. 5 displays i^{-1} *vs.* $\omega^{-0.5}$ plots for various potentials in the hydrogen region of the Pt(*hkl*); these plots for various potentials in the anodic hydrogen overpotential region yields straight lines with the intercept corresponding to the kinetically controlled current (i_k^{-1}), and the slope corresponding to the mass-transfer factor B^{-1}. Note that at the same potential, $i_k(111) \approx i_k(100) \ll i_k(110)$ which indicates the order of absolute kinetic activity of the three surfaces. At sufficiently anodic potentials, different for each of the surfaces, the lines go through the origin, indicating that at these potentials the HOR is a purely diffusion limited reaction. Levich–Koutecky plots for the (100) surface in the OH_{ads} potential region are shown in Fig. 6; these plots reveal that the slope (the mass-transfer factor B) is essentially the same as that measured in the low overpotential region.

Fig. 7 shows so-called 'Tafel plots', log i *vs.* E, at low overpotentials from the polarization curves at 3600 rpm (Fig. 4), where measured current densities are essentially due entirely to kinetic resistance for the HER and HOR. For all three surfaces, the Tafel slopes, d log i/dE, increased monotonically with the overpotential. Depending on the fitting method, *i.e.*, the method of drawing the tangent through the points of what appears to be a continuous curve, one might extrapolate any Tafel slope between *ca.* 50 and 150 mV (decade)$^{-1}$. In our case, for Pt(110) we fitted the curves with two slopes: a low Tafel slope *ca.* 55 mV (decade)$^{-1}$ and high Tafel slope with 140 mV (decade)$^{-1}$. Note that (110) is the only surface with a symmetrical log i *vs.* E relationship, indicating that there is a single exchange current density for the hydrogen electrode reaction applicable to both anodic and cathodic processes (*ca.* 7×10^{-4} A cm^{-2}). On Pt(100) the HER appears to have two Tafel slopes; at low overpotentials *ca.* 65 mV (decade)$^{-1}$ and at high overpotentials *ca.* 140 mV (decade)$^{-1}$. This surface also has the most asymmetrical curves, with significantly higher exchange current density for the HER (*ca.* 4×10^{-4} A cm^{-2}) than for the HOR (*ca.* 5×10^{-5} A cm^{-2}). The (111) surface does not have a transition in Tafel slope that can be defined in a consistent way. On this surface, the exchange

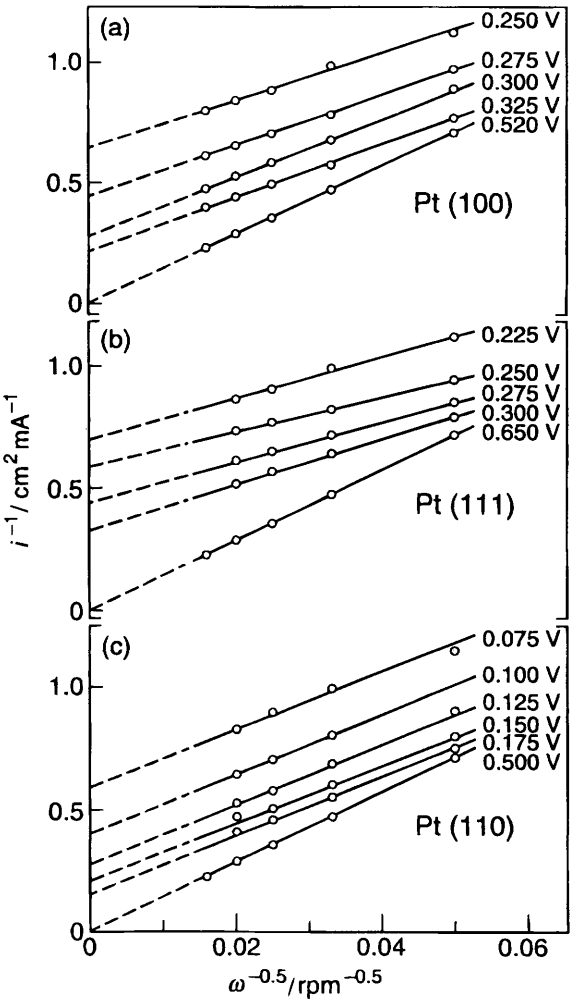

Fig. 5 Levich–Koutecky plots for the HOR on Pt(*hkl*) at various electrode potentials in the hydrogen underpotential region

current density for the HOR (*ca.* 4×10^{-5} A cm^{-2}) is lower than for the HER (*ca.* 7×10^{-5} A cm^{-2}). Our results for the (110) surface are comparable to those reported for polycrystalline Pt in the relatively few reports of work in alkaline solution. For the HER on polycrystalline platinum electrode in 0.5 M NaOH, Conway *et al.*[23] and Bai *et al.*[24] reported a Tafel slope of 75 mV (decade)$^{-1}$ in the low overpotential range, and a value of 125 mV (decade)$^{-1}$ at high over-

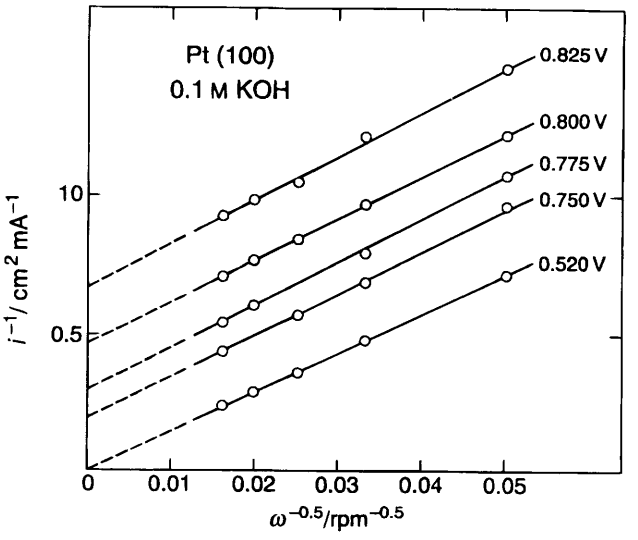

Fig. 6 Levich–Koutecky plots for the HOR on Pt(100) at various electrode potentials in the hydroxy adsorption region

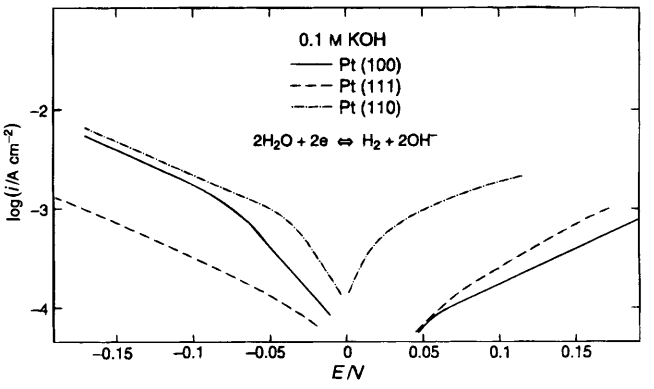

Fig. 7 Tafel plots for the HER and HOR on Pt(*hkl*) in 0.1 M KOH at 3600 rpm

potentials. Bagotsky and Osterova reported an exchange current density of *ca.* 0.1 mA cm^2 for polycrystalline Pt in 0.5 M NaOH.[10]

4. Discussion

Polarization curves for the HER and HOR on Pt single-crystal surfaces in alkaline solution clearly show that the kinetics of hydrogen reaction is strongly affected by the symmetry of Pt surface atoms. Although it has long been recognized that some electrode reaction rates are a function of the crystallographic orientation of Pt(*hkl*) (two prominent examples being the oxidation of small organic molecules[25] and the reduction of oxygen[15,16]), our results demonstrate, for the first time, that the kinetics of HER and HOR on Pt(*hkl*) in alkaline solution are also sensitive to the surface structure. Because the adsorption isotherm for hydrogen in the overpotential region, H_{upd}, is strongly dependent on crystal face, it is obvious that one would first seek a rationalization of the structure sensitivity of the HOR (at least) in terms of H_{upd} and its role in the rate determining step (rds). We present here an interpretation of the kinetics of HOR and HER on Pt(*hkl*) in alkaline solution based on the proposition that differences arise mainly from the structure sensitivity of H_{upd} and OH_{ads} on Pt(*hkl*) and their roles in the mechanism of the reaction.

4.1 The mechanism of the HOR on Pt(*hkl*)

The HOR on platinum electrode is usually assumed to proceed by a mechanism which involves initial adsorption of molecular hydrogen with simultaneous dissociation of the molecule into atoms

$$H_2 \underset{\text{rds}}{\longleftrightarrow} 2H_{ad} \qquad (2)$$

followed by adsorbed atomic hydrogen ionization

$$H_{ad} + OH^- \rightleftharpoons H_2 + e^- \qquad (3)$$

i.e., historically referred to in some accounts as the Tafel–Volmer sequence.[1] It should be noted that the H_{ad} is not the same species as the H_{upd}, as we discuss below.

As shown for the polycrystalline platinum electrode in alkaline solution,[10] the rate of the second step is much larger than that of the first, the dissociative hydrogen adsorption [eqn. (2)] being thus the rate determining step of the total process. Although there may be some consensus about reactions (2) and (3), the question of whether underpotentially deposited hydrogen, H_{upd}, usually observed by cyclic voltammetry in the absence of molecular hydrogen, is identical to the hydrogen states formed from step (2) (*e.g.*, H_{ad}) is controversial. Also, it is important to know whether the sites for dissociation are the same as the sites for ionization (or is dissociation followed by rapid surface diffusion to a different site where ionization takes place?). Thus, there are many different rate expressions one could write even for the simple mechanism represented by reactions (2) and (3). By using a more empirical analysis, however, we are able to examine the relationship between H_{upd} and the reaction kinetics.

4.1.1 Effects of H_{upd}. By using single crystals of Pt, we gain considerable insight into the relationship between H_{upd} coverage and the kinetics because the three different crystal faces have three very different isotherms for H_{upd} and very different reactivities for the HOR. A comparison of the anodic part of the polarization curves in Fig. 4 with the adsorption isotherms for H_{upd} in Fig. 2 clearly shows that on Pt(110) the HOR occurs even on a surface which is 'fully' covered by the H_{upd} (1 ML = 147 μC cm^{-2}). On both Pt(100) and (111), however, the onset of comparable current density appears to be correlated with the desorption of a significant amount of H_{upd}, and thus the creation of a critical number of 'bare' Pt sites. The influence of H_{upd} on the kinetics of HOR is most pronounced for the Pt(111) surface, as shown in Fig. 2 and 4. It is important to note that the (111) surface covered by $H_{upd} > 0.5$ ML is almost completely inactive for the HOR. Therefore, given that the increase in the rate of HOR on all three platinum single-crystal surfaces is mirrored by a decrease in coverage of H_{upd}, we can write a rate expression based on steps (2) and (3) using H_{upd} as the only state adsorbed on the surface. Since the dissociation of molecular hydrogen is a chemical reaction, the potential dependence of the rate comes entirely from step (2), and hence, entirely from the potential dependence of the surface coverage by H_{upd}. We do not claim that our analyses here is definitive. In fact, it is just a model relating the oxidation rate (in the absence of any mass transfer effects) for hydrogen molecules on Pt(*hkl*) to the availability of 'bare' platinum sites $(1 - \theta_{H_{upd}})$. Since we do not know the details of the site-blocking interaction between H_{upd} and the dissociation of H_2, we will use an empirical relation between the number of 'bare' Pt sites available for H_2 dissociation and H_{upd} given by

$$i_{k,ox} = i_{\theta_{H_{upd}}=0}(1 - \theta_{H_{upd}})^m \qquad \text{(III)}$$

Integral values of $m = 1$ or 2 would correspond to ideal (Langmuirian) single- or dual-site blocking interactions by H_{upd}. Then, we can write the rate of the rds [step (2)] using a simple chemical rate expression

$$\log i_{k,ox} = \log i_{\theta_{H_{upd}}=0} + m \log(1 - \theta_{H_{upd}}) \qquad \text{(IIIa)}$$

Note again that the potential dependence arises solely from the potential dependence of H_{upd}. Plotting the kinetically controlled currents as $\log i_{k,ox}$ *vs.* $\log(1 - \theta_{H_{upd}})$ produces a linear relationship for all three surfaces, as shown in Fig. 8. From the slope of the straight line, one can evaluate the exponent $m_{Pt(hkl)}$ and this gives $m_{Pt(111)} = 2$, $m_{Pt(100)} = 1.5$ and $m_{Pt(110)} = 0.5$. From this analysis it appears that the HOR on Pt(111) in alkaline solution follows the ideal dual-site form of the Tafel–Volmer sequence. The same functionality might also apply to Pt(100), although the m is not exactly equal to 2. It is possible that the decrease of the current density of HOR does not match perfectly with the number of pairs of (100) sites because some (unknown) fraction of H_{upd} on (100) may lie below the surface plane, as indicated by our X-ray scattering measurements[17,†] and therefore does not block H_2 disso-

† We should note that X-ray scattering measurements are not sensitive to the location of hydrogen atoms on or below the surface. The X-ray measurements, however, accurately measure the expansion of the surface platinum atoms as a function of electrode potential. The Pt(100) surfaces showed a large (>5%) expansion in the H_{upd} region and this could be consistent with the presence of subsurface hydrogen. In contrast, the Pt(111), showed a considerably smaller expansion (0–1.5%) in the H_{upd} region.

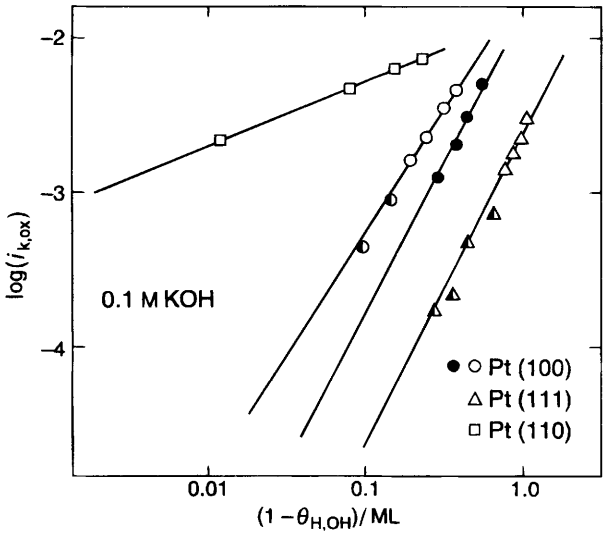

Fig. 8 Plots of log $i_{k,ox}$ *vs.* log$(1 - q_{H,OH})$. (○, △) are points inferred from Fig. 2 and 5 in the H_{upd} region; (●, ▲) are points inferred from Fig. 2 and 6 in the OH_{ad} region; (◐, ◭) are points inferred in H_{upd} region (Fig. 2 and 4) where HOR is a purely kinetically controlled process.

ciation. On the other hand, the X-ray scattering measurements for Pt(111) show much less subsurface hydrogen (if any at all).

The (110) surface does not fit very well to our model, in the sense that $m = 0.5$ does not have a physical meaning. Together with the simple observation made above, that the surface is very active even when coverage by H_{upd} is complete, it is our conclusion that there are sites for H_2 dissociation on the (110) surface that are not occupied by H_{upd}, although a full monolayer of hydrogen is adsorbed. In our recent study of the ORR on Pt(110), we noted that the (110) surface is very open and, therefore, that even if it is 'fully' covered by H_{upd} there might still be available bare platinum atoms that can serve as sites for O—O bond breaking.[16] An analogous situation could be applied to the adsorption of molecular H_2 on the (110) sites and the subsequent H—H bond breaking. Until recently, relatively little was known about the true nature of adsorbed H_{upd} on Pt(110) in solution. Also the real structure [*i.e.*, (1 × 1) or reconstructed surface] of the Pt(110) surface prepared by flame annealing in hydrogen was also unknown. Our most recent X-ray scattering measurements for Pt(110) clearly show that the surface prepared by flame annealing, followed by cooling in hydrogen, exhibits a very stable (1 × 2) reconstruction that is present in alkaline solution over a wide potential range, and is only removed when the surface is roughened by irreversible oxidation.[19] Furthermore, the results suggested that the most plausible adsorption sites for H_{upd} are the three-fold coordinated sites below the top-most (110) rows of Pt atoms, as shown in Fig. 1(c). A pronounced relaxation of the top-most atomic rows (*ca.* 20%) outward from the underlying atoms was observed in the potential region of the H_{upd}, indicating that a significant fraction of the H_{upd} might be below the surface. If we assume that H_2 adsorption and dissociation can occur on the top sites of the Pt(110) (1 × 2) surface, see insert of Fig. 1(c), then it is possible that even when the electrode is 'fully' covered with H_{upd}, the oxidation reaction can still proceed at a high rate. The model that appears to rationalize the results for the HOR at low anodic overpotentials on all Pt single-crystal surfaces is one where the underpotential deposited hydrogen, H_{upd}, is a strongly bound state ($\Delta_{ad}G < 0$) but the active intermediate, H_{ad}, is a low binding energy state ($\Delta_{ad}G > 0$).

4.1.2 Effects of OH_{ads}. At high overpotentials, *i.e.*, in the potential region where platinum surface atoms are partially covered by OH_{ad}, the activity of Pt(*hkl*) for the HOR decreases in the sequence (111) > (110) > (100). Interestingly, the rate of the HOR on Pt(111) is not measurably affected by the coverage of OH_{ad} for the reversible state adsorbed in the anomalous potential region. The decrease in an activity above *ca.* 0.9 V coincides with the onset of the formation of the surface 'oxide' by the place-exchange mechanism.[26] The lack of sensitivity of the HOR reaction on the (111) surface is very interesting, but it is difficult to attribute a unique physical meaning to it. The simplest physical model which might describe the effects of OH_{ad} on the kinetics of HOR, interpreted in terms of the Tafel–Volmer sequence, could be the same as in the case of ORR,[16,†] *i.e.*, the lack of sensitivity of the HOR at high anodic overpotentials would imply that reversibly adsorbed OH_{ad} on (111) does not block sites for dissociative adsorption of H_2.

On (100), the dissociative adsorption of H_2 molecules is inhibited even at low surface coverage by OH_{ad}. The 'bell-shape' of the polarization curves for Pt(100) in Fig. 3, *e.g.*, the curves in the OH_{ad} region are almost a mirror image of the curves in the H_{upd} region, imply that the reversible adsorption of hydroxide ions suppresses activity in nearly the same way as H_{upd} does. Thus, it appears that on Pt(100) the effects of OH_{ad} on the HOR could be analogous to that proposed above for H_{upd}. Using i_k determined from the *y*-intercepts of the Levich–Koutecky plots in Fig. 6, and from the adsorption isotherm of the OH_{ad} shown in Fig. 2, assuming complete discharge of the OH ion, we have plotted the functionality of log $i_{k,ox}$ *vs.* log$(1 - \theta_{OH})$ in Fig. 8. The resulting relationship is linear and the slope of the straight line, $m_{Pt(100),ox} = 2$. This implies that the current density of the HOR on Pt(100) in the OH_{ad} region decreases to the second power, *i.e.*, unoccupied Pt-pair sites are required for the dissociative chemisorption of H_2. The occurrence of the ideal exponent, $m = 2$, for Pt(100) in the OH_{ad} region *vs.* the non-ideal value of 1.5 in the H_{upd} region might be interpreted as indicating that OH_{ad} at submonolayer coverage is adsorbed onto the (100) surface rather than in or below the surface, consistent with physical models of OH_{ad} based on other data.[26]

4.2 The mechanism of the HER on Pt(*hkl*)

We will assume that the mechanism for the HER is the same as for the HOR, since we are analysing the HER only at low overpotentials. The adsorbed intermediate, designated as H_{opd} for the overpotential region, is formed cathodically from the reduction of H_2O rather than from the dissociation of H_2 as in the HOR. The reduction of water

$$H_2O + e^- \rightleftharpoons H_{opd} + OH^- \quad (4)$$

is coupled with removal of H_{opd} by a recombination step

$$2H_{opd} \xrightarrow[rds]{} H_2 \quad (5)$$

Unfortunately, relatively little is known about the true nature of H_{opd} in electrolytic solutions. Conway and co-workers[24] proposed that H_{opd} is uniquely different from H_{upd}, and that its coverage in the hydrogen evolution potential region could be calculated from potential decay transients. From IR spectroscopic measurements Nichols and Bewick[27] observed that at potential below 0.08 V a new vibrational band shifted from that for H_{upd} on polycrystalline Pt and on Pt(111) in 1 M H_2SO_4. By correlating the potential dependence of the band intensity with the rate of hydrogen evolution they concluded that this adsorbed hydrogen is the reaction intermediate in the HER, in our notation H_{opd}.

Our results clearly show that the HER on Pt(*hkl*) in 0.1 M KOH is a structurally sensitive process, with the order of

† It appears that due to weak adsorption and high mobility of the OH_{ad} species on the (111) surface, the adsorption of molecular O_2 (the proposed rds) is not blocked by these species.

activity of Pt(*hkl*) increasing in the sequence (111) < (100) < (110). In the discussion which follows, we present an admittedly speculative rationalization for the differences in activity with crystal face in terms of differences in the nature of adsorbed hydrogen and the role of adsorbed hydrogen in the formation of 'bare' Pt sites, which are required for a rate determining chemical recombination step to take place. Following our interpretation of the HOR, we propose that during the HER two different types of hydrogen can be distinguished on Pt(*hkl*); strongly adsorbed hydrogen, H_{upd}, (*e.g.*, high bonding states, $\Delta_{ad}G < 0$) is a spectator species (site blocking) in the HER, and weakly adsorbed hydrogen, H_{opd}, (*e.g.*, low bonding states, $\Delta_{ad}G > 0$) is the reaction intermediate in HER. For Pt(110), at low cathodic overpotentials the H_{upd} is adsorbed in the 'troughs' of the (1 × 2) structure, thus leaving the top Pt-pair sites available for the reaction of recombination of the adsorbed H_{opd}. We note that steps (4) and (5) occur even when the (110) surface is 'fully' covered by the H_{upd}, as was the case of the HOR at low positive overpotentials. Assuming that on either side of the equilibrium potential for the hydrogen reaction the (110) surface always provides the same number of active centres (pair of Pt sites), then the kinetics of the HER and HOR should be comparable, as confirmed from the symmetrical shape of the Tafel plots in Fig. 7, and by the fact that the same value for the exchange current densities for the HER and HOR are observed. On the Pt(100) surface, we postulate that at low anodic overpotentials the top Pt sites are completely blocked by H_{upd}. The result is that unoccupied Pt-pair sites on Pt(100), required for the recombination of H_{opd}, can only be created if some amount (unknown) of the H_{upd} moves to a subsurface state when the potential is made more negative. Therefore, the surprising anodic/cathodic asymmetry for the polarization curves (Tafel plots) for the (100) surface can be rationalized as arising from a transition in the nature of H_{upd} and its effect on kinetics in two different potential regions. The least active surface for the HER is the Pt(111) surface. Our X-ray scattering results[17] have shown that this surface forms much less subsurface hydrogen than (100) in the same potential region, and, therefore, the site for hydrogen recombination remains highly blocked by H_{upd}. Our fundamental rationale for all Pt surfaces is that in order to have an appreciable rate of the HER some of the H_{upd} has to be in a subsurface state in order to allow the formation of a pair of 'bare' platinum sites which can be occupied by intermediate H_{opd}.

5. Conclusions

On the basis of results presented above, and in harmony with the discussion in ref. 9, it is reasonable to conclude that the adsorbed state of hydrogen that is the active intermediate in both the HER and HOR at low overpotentials on all Pt surfaces is a low binding energy state ($\Delta_{ad}G > 0$). In contrast, the more strongly bound state of the adsorbed hydrogen, H_{upd}, which is thermodynamically equivalent to an underpotential state ($\Delta_{ad}G < 0$), is not an active intermediate and has a site blocking effect. Consequently, at low overpotentials, the potential dependence of the rates of the HER and HOR arise primarily from the potential dependence of the isotherm for the low binding energy state, the chemical recombination step being rate determining. The (110) surface, possibly by virtue of its surface geometry, has the most favourable isotherm for the low energy state and the most facile kinetics of the low index faces of Pt.

We would like to thank Chris Lucas for helpful discussion and suggestions and Lee Johnson and Frank Zucca for their invaluable help in polishing the single crystals and setting up of the experimental apparatus. This work was supported by the Assistant Secretary for Conservation and Renewable Energy, Office of Transportation Technologies, Electric and Hybrid Propulsion Division of the U.S. Department of Energy under Contract No. DE-AC03-76SF00098.

References

1 K. J. Vetter, *Electrochemical Kinetics*, ed. S. Bruckensein and B. Howard, Academic Press, New York, 1967, pp. 516–614.
2 J. O'M Bockris and A. K. Reedy, *Modern Electrochemistry*, Plenum Press, New York, 1983, vol. 2.
3 B. E. Conway and J. O'M. Bockris, *J. Chem. Phys.*, 1957, **26**, 532.
4 R. Parsons, *Trans. Faraday Soc.*, 1958, **54**, 1053.
5 H. Gerisher, *Bull. Soc. Chim. Belg.*, 1958, **67**, 506.
6 L. I. Krishtalik, in *Advances in Electrochemistry and Electrochemical Engineering*, ed. P. Delahay and C. W. Tobias, John Wiley & Sons, New York, 1970, vol. 7.
7 S. Trasatti, in *Advances in Electrochemistry and Electrochemical Engineering*, ed. H. Gerisher and C. W. Tobias, John Wiley & Sons, New York, 1977, vol. 10.
8 S. Trasatti, *J. Electroanal. Chem.*, 1977, **39**, 183.
9 E. Protopopoff and P. Marcus, *J. Chim. Phys.*, 1991, **88**, 1423.
10 V. S. Bagotzky and V. Osterova, *J. Electroanal. Chem.*, 1973, **43**, 233.
11 S. Schulander, M. Rosen and D. Flinn, *J. Electrochem. Soc.*, 1970, **117**, 1251.
12 K. Seto, A. Iannello, B. Love and J. Lipkowski, *J. Electroanal. Chem.*, 1987, **226**, 351; H. Kita, S. Ye and Y. Gao, *J. Electroanal. Chem.*, 1992, **334**, 351.
13 R. Gomez, A. Fernandez-Vega, J. M. Felui and A. Aldaz, *J. Phys. Chem.*, 1993, **97**, 4769.
14 M. Breiter and R. Clamroth, *Z. Elektrochem.*, 1954, **58**, 4933; M. Breiter, C. Knorr and R. Meggle, *Z. Elektrochem.*, 1955, **59**, 153.
15 N. M. Marković, H. A. Gasteiger and P. N. Ross, *J. Phys. Chem.*, 1995, **99**, 3411.
16 N. M. Marković, H. A. Gasteiger and P. N. Ross, *J. Phys. Chem.*, 1996, **100**, 6715.
17 I. M. Tidswell, N. M. Markovic and P. N. Ross, *Phys. Rev. Lett.*, 1993, **71**, 1601.
18 I. M. Tidswell, N. M. Markovic and P. N. Ross, *J. Electroanal. Chem.*, 1994, **376**, 119.
19 C. A. Lucas, N. M. Markovic and P. N. Ross, *Phys. Rev. Lett.*, in the press.
20 E. Kirsten, G. Parschau, W. Stocker and K. I. Rieder, *Surf. Sci.*, 1990, **231**, L183.
21 M. Breiter, C. A. Knorr and W. Vôlkl, *Z. Elektrochem.*, 1955, **59**, 681.
22 F. Ludwig, R. K. Sen and E. Yeager, *Electrochemiya*, 1997, **13**, 847.
23 B. E. Conway and L. Bai, *J. Electroanal. Chem.*, 1986, **198**, 149.
24 L. Bai, D. A. Harrington and B. E. Conway, *Electrochim. Acta*, 1987, **32**, 1713.
25 N. M. Marković and P. N. Ross, *J. Electroanal. Chem.*, 1992, **330**, 499.
26 F. Wagner and P. Ross, *Surf. Sci.*, 1985, **160**, 305.
27 R. Nichols and A. Bewick, *J. Electroanal. Chem.*, 1988, **243**, 445.

Paper 6/02575G; *Received* 12*th April*, 1996